Lower-Tropospheric Humidity–Temperature Relationships in Radiosonde Observations and Atmospheric General Circulation Models

REBECCA J. ROSS, WILLIAM P. ELLIOTT,* AND DIAN J. SEIDEL

NOAA Air Resources Laboratory, Silver Spring, Maryland

PARTICIPATING AMIP-II MODELING GROUPS+

(Manuscript received 6 February 2001, in final form 14 August 2001)

ABSTRACT

Annual and seasonal correlations between temperature and both specific and relative humidity are presented based on radiosonde station data over the tropical Pacific Ocean and North America. Results are presented for the surface and the 850-, 700-, and 500-hPa levels. The correlations between anomalies of temperature and relative humidity are generally negative, and those between temperature and specific humidity are generally positive. Longitudinal differences in the pattern of correlations are found both in low latitudes and over midlatitude North America. In particular, near-zero or negative temperature–specific humidity correlations are found in the western United States at and below 700 hPa (especially in summer) and over the western tropical Pacific at 700 and 500 hPa (especially in winter). The observed correlation patterns are compared with those of 12 atmospheric general circulation model (AGCM) simulations. Simulated high-latitude correlation patterns qualitatively agree with observations, but a sizable fraction of the correlations are higher than observed. The models show varying degrees of success in simulating the longitudinal differences in the temperature–specific humidity relationship in midlatitudes. At low latitudes, the models are generally unsuccessful at simulating the observed longitudinal differences. The simulated mean humidity fields are also compared with observations. The models show 10%–20% higher relative humidity than is observed at mid- and high latitudes and over the Tropics. However, over the Pacific region, the relative humidity bias is of opposite sign (models drier than observed) and is confined to the 850-hPa level.

1. Introduction

This paper examines correlations between anomalies of temperature and anomalies of specific and relative humidity as observed by radiosondes. Of particular interest here are variations in the temperature–humidity relationship between different geographical regions and by season. The paper also compares the observed temperature–humidity relationships with those simulated by AGCMs. Among the most important positive climate feedback mechanisms in AGCMs is that due to tropospheric water vapor (e.g., Hall and Manabe 1999; Garratt et al. 1999). Surface and tropospheric warming lead to enhanced tropospheric specific humidity, which, by virtue of the greenhouse effect of water vapor, further warms the surface. Here, model simulations from the second Atmospheric Model Intercomparison Project (AMIP II) are examined to determine how well the models simulate the observed joint distributions of temperature and humidity. This comparison provides a second-order test of the models beyond the evaluation of simulated monthly means. Deficiencies in the simulated temperature–humidity relationship may indicate deficiencies in the water vapor feedback and more generally in the accuracy of the climate simulation.

Two idealized examples of the temperature and water vapor relationship can be imagined: 1) a constant specific humidity q as temperature T changes, in which case the T–q correlation would be zero while the correlation of temperature and relative humidity RH would be strongly negative, and 2) a constant relative humidity as temperature changes, in which case the T–RH correlation would be zero while that between temperature and specific humidity would be strongly positive. Although neither of these two idealizations explains the observed relationship, they can be starting points for examining the relationships between temperature and humidity anomalies both in the atmosphere and in AGCMs.

Randel et al. (1996) and Wentz and Schabel (2000)

* Retired.

+ List of participating AMIP-II modeling groups is given in Table 1.

Corresponding author address: Dian Seidel, NOAA Air Resources Laboratory R/ARL, 1315 East West Highway, Silver Spring, MD 20910.
E-mail: dian.seidel@noaa.gov

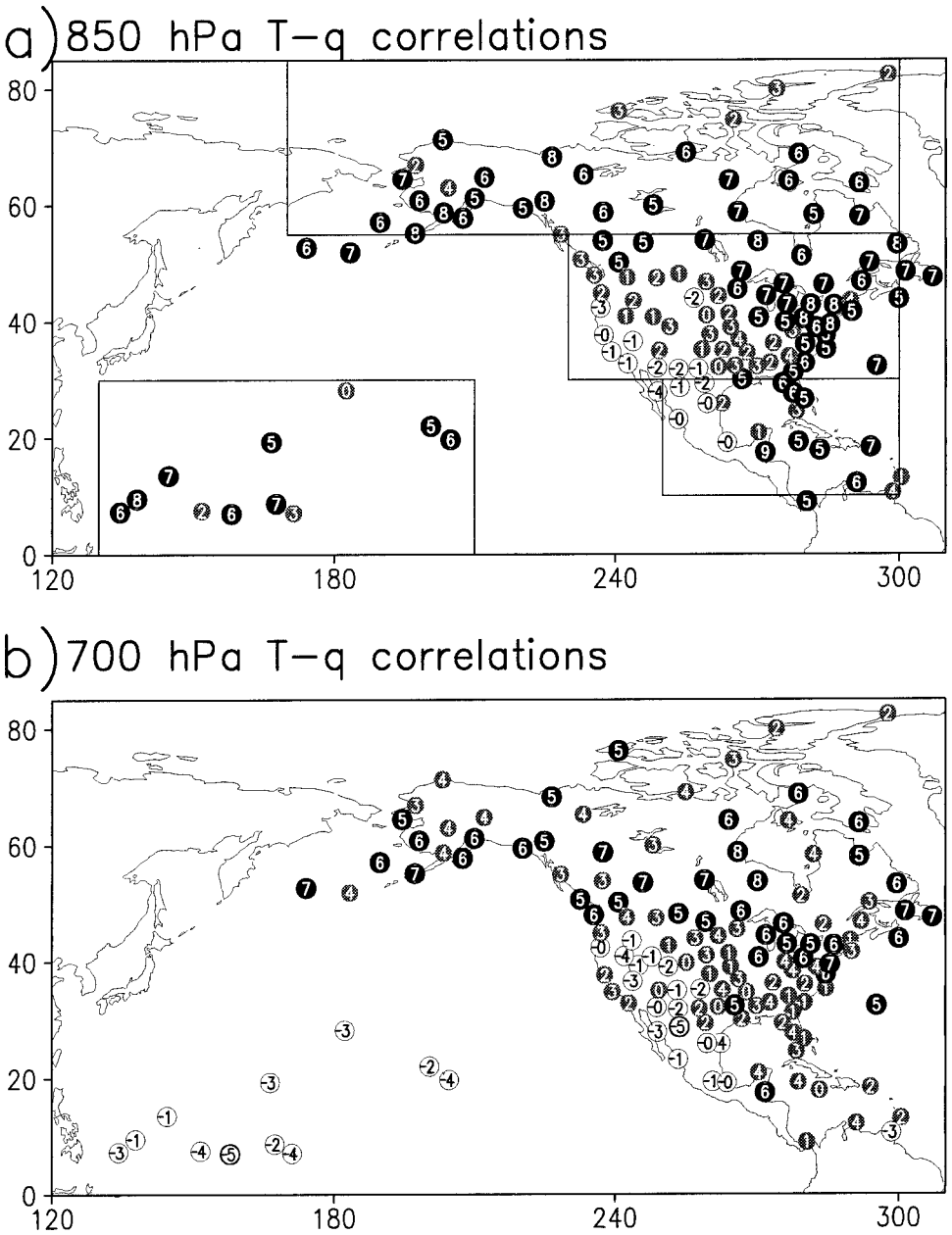

FIG. 1. Spearman correlation coefficients (×10 and truncated) between annual anomalies of temperature and specific humidity at (a) 850 and (b) 700 hPa. Positive correlations are shown by white numbers on gray or black circles, where black circles indicate the correlation is significant (i.e., >0.50). Negative correlations are shown by black numbers on white circles, and significant negative correlations are indicated by the thicker black circumference of the circles. The rectangular areas are the boundaries of the regions in which the model simulations were sampled for comparison with the observations.

have shown that, on a global, hemispheric, and zonal average, interannual variations of column-integrated water vapor (precipitable water) and both surface and lower tropospheric temperature are correlated well. In general, the positive correlation between surface temperature and precipitable water is also evident locally (Stephens 1990; Inoue 1990; Gaffen et al. 1992a; Bony et al. 1995). However, about one-half the precipitable water resides within the first 1.5 km above the surface, and the high correlation between surface temperature and precipitable water, over large regions and locally, may be largely a boundary layer phenomenon. As shown by Hu (1996) and Held and Soden (2000), the radiative impact of water vapor in the free troposphere is larger than that in the boundary layer. Therefore, the relationships between tempera-

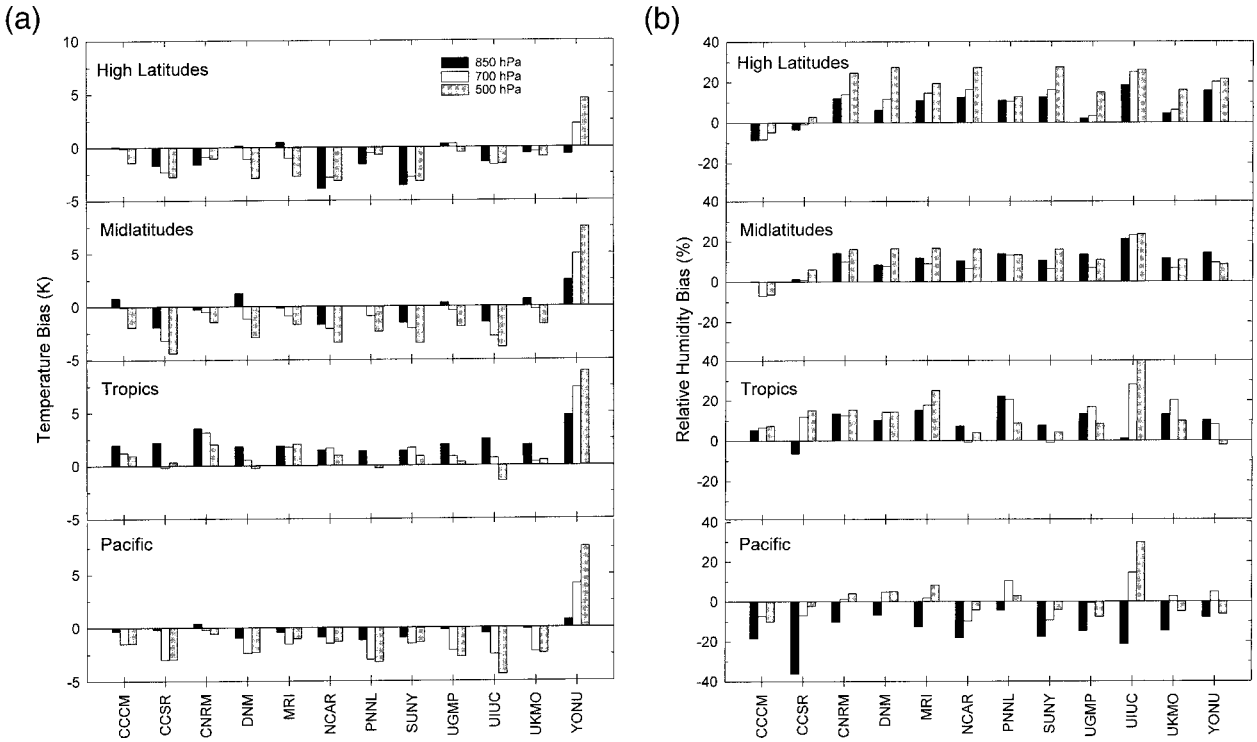

FIG. 2. Differences (AGCM simulation minus radiosonde observations) in climatological annual and regional mean (a) temperature and (b) relative humidity. For each model, there are three bars representing the differences at 850 (left black bar), 700 (middle white bar), and 500 hPa (right gray bar).

ture and water vapor in the free troposphere are directly relevant to understanding the water vapor climate feedback mechanisms.

Sun and Oort (1995) investigated the vertical structure of relationships between temperature and humidity averaged over the tropical belt (30°N–30°S). Using radiosonde data from 1968 through 1989, they found positive correlations between detrended zonally averaged monthly anomalies of q and T from the surface up to 300 hPa, and negative correlations between RH and T. Using the same radiosonde dataset and averaging over the tropical belt, Sun and Held (1996) found that the observed positively correlated q and T anomalies in the troposphere are weaker than those simulated by the Geophysical Fluid Dynamics Laboratory AGCM. However, Hu et al. (2000) find the National Center for Atmospheric Research Community Climate Model, version 3, slightly underestimates the tropical T–q relationship when compared with reanalysis. These results bear on the sensitivity of the climate system and AGCMs to an external forcing and thus on the reliability of climate predictions based on AGCM experiments.

Our examination of the observed and simulated relationships among T, q, and RH anomalies is in contrast to the approach of Sun and Oort (1995) and Sun and Held (1996) in that we examine these relationships at individual stations rather than in zonal averages, with emphasis on isolating longitudinal and latitudinal variations, both within the Tropics and at more northerly latitudes. Section 2 describes the analysis methods, including the radiosonde data and AGCM simulations used and the statistical computations. Section 3 presents relationships among T, q, and RH, at four tropospheric levels, for both the observations and simulations, and section 5 summarizes the main findings and discusses their implications.

2. Data and methods

a. Radiosonde data

Radiosonde temperature and humidity soundings for 1979–95 from 150 stations operated by the United States and Canada, shown in Fig. 1, form the observational dataset for this investigation. The network was chosen because VIZ Manufacturing Company radiosondes were used for many years in the United States and Canada and so the humidity data are homogeneous during the period of analysis (Gaffen 1996). Data from 17 U.S. stations that used the Space Data Division radiosonde in the late 1980s and early 1990s were adjusted for an error in the humidity data processing algorithm (Wade 1994) by using the technique described by Elliott et al. (1998).

From each sounding, T, q, and RH at the surface and at the 850-, 700-, and 500-hPa levels were extracted or

TABLE 1. Atmospheric general circulation models, from the Atmospheric Model Intercomparison Project II, used in this study, their grid spacing (lat × long), and their vertical levels. More information about the models was available at the time of writing on the AMIP Web page at http://www-pcmdi.llnl.gov/modeldoc/amip2/index.html.

Modeling group	Model acronym	Grid spacing	Vertical levels
Canadian Centre for Climate Modelling and Analysis, Victoria, Canada	CCCM	~3.7° × 3.75°	32
Center for Climate System Research, Tokyo, Japan	CCSR	~2.8° × 2.8°	18
Centre National de Recherches Météorologiques, Toulouse, France	CNRM	~2.8° × 2.8°	45
Department of Numerical Mathematics, Russian Academy of Sciences, Moscow, Russia	DNM	4° × 5°	21
Meteorological Research Institute, Ibaraki-ken, Japan	MRI	~2.8° × 2.8°	30
National Center for Atmospheric Research, Boulder, CO	NCAR	~2.8° × 2.8°	18
Pacific Northwest National Laboratory, Richland, WA	PNNL	~2.8° × 2.8°	18
University at Albany, State University of New York, Albany, NY	SUNY	~2.8° × 2.8°	18
University of Illinois at Urbana–Champaign, Champaign, IL	UIUC	4° × 5°	24
Hadley Centre for Climate Prediction and Research, Met Office, Bracknell, United Kingdom	UKMO	2.5° × 3.75°	19
UK Universities Global Atmospheric Modelling Programme, Reading, United Kingdom	UGAMP	2.5° × 3.75°	58
Yonsei University, Seoul, Korea	YONU	4° × 5°	15

calculated using the quality-control procedures described by Ross and Elliott (1996a). Monthly means and anomalies (deviations from the 1979–95 monthly average) were computed for each station and level. Seasonal (December–January–February, etc.) and annual anomalies were calculated by averaging the monthly anomalies. Separate monthly, seasonal, and annual anomaly time series were created from 0000 and 1200 UTC observations. However, the results based on each time were not very different, particularly above the surface. Therefore, we present only 0000 UTC results below, because more stations reported at 0000 than at 1200 UTC.

There were several reasons to confine the analysis to observations at 500 hPa and below. Besides the lower reliability of humidity observations at cold temperatures (Elliott and Gaffen 1991), two practices were in effect at U.S. sites during this period that could affect temperature–humidity correlations at higher levels. When temperatures fell below −40°C, the United States reported the humidity as ''missing,'' regardless of its measured value. Most of these cold observations occur above 500 hPa, and any correlations based on data ensembles with missing humidity in cold conditions would be suspect. Furthermore, from 1973 until 1993, the United States coded a dewpoint depression of 30°C when the relative humidity was less than 20%. These dry observations are more numerous at high levels but can be found elsewhere, particularly at stations along the west coast of the United States and in the central Pacific (Ross and Elliott 1996b). It has been our practice to use a value of 16% for the RH in these cases, and this assumption, too, could have a small effect on the correlations.

b. Model simulations

Atmospheric GCM simulations from the AMIP-II project (e.g., AMIP Newsletter No. 8, available online at the time of writing at http://www-pcmdi.llnl.gov/amip/NEWS/amipnews.html) cover the period of 1979–95. AMIP-II protocols specify the model boundary conditions and forcings (e.g., sea surface temperature, sea ice, greenhouse gas concentrations, solar radiation), which were based on observational data. Although about 35 models are expected to produce simulations for AMIP II, not all simulations are available yet. We have used the 12 available simulations from models listed in Table 1. Each model grid point was treated in the same manner as the radiosonde station data. Monthly, seasonal, and annual anomalies of *T*, RH, and *q* were computed for the 850-, 700-, and 500-hPa levels.

For comparison with the radiosonde observations, we sampled the model output at all grid points within rectangular regions defined by the radiosonde station locations and shown in Fig. 1. We define three latitude bands based on the observed correlation patterns: high latitude (55°–90°N), midlatitude (30°–55°N), and low latitude (0°–30°N), but note that the longitudinal extent of each band is limited by the radiosonde locations within the longitudinal boundaries 130°–310°E (50°W). The midlatitude band is further subdivided (at 265°E) into western and eastern U.S. regions. The low-latitude region is also the union of two subregions, the region over

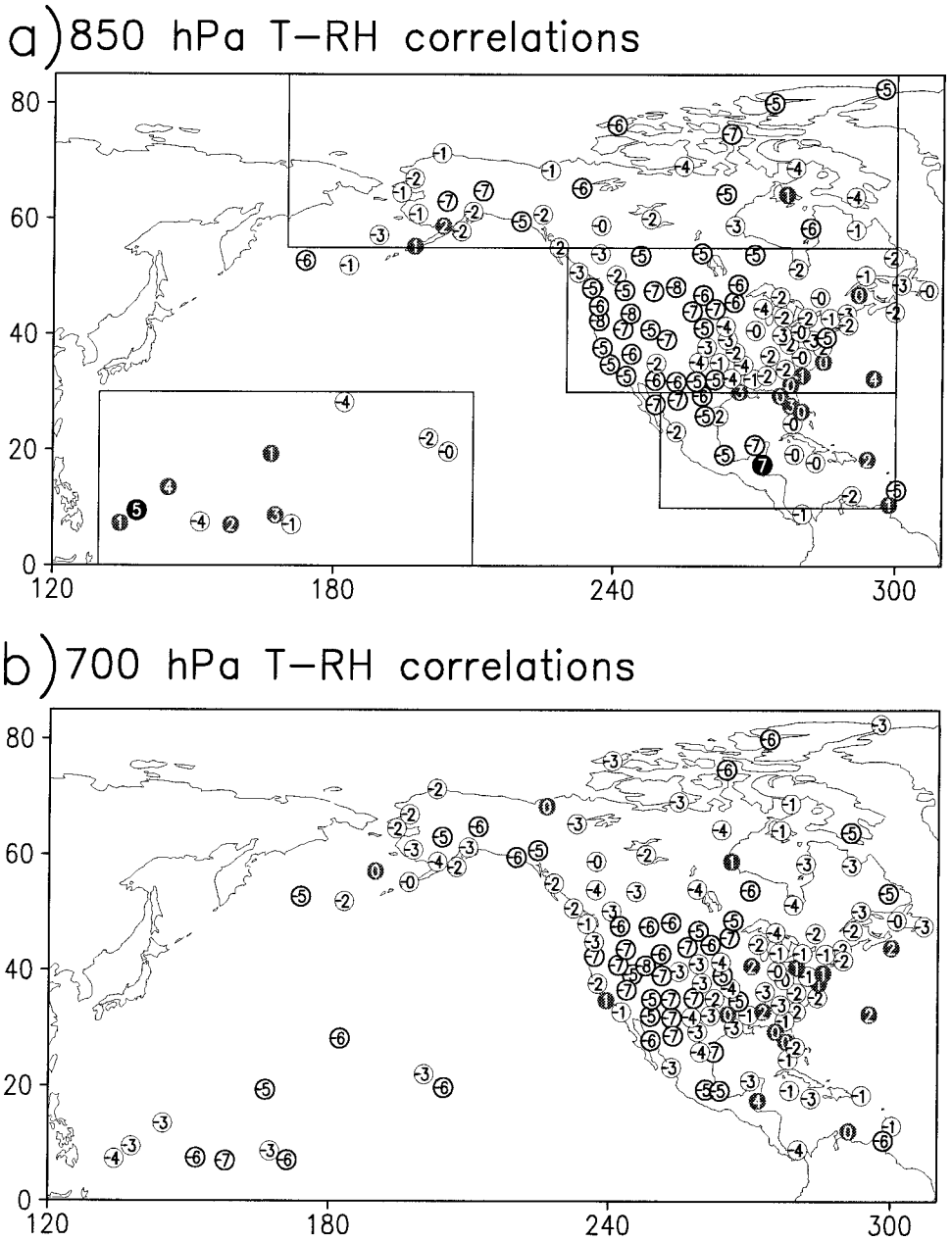

FIG. 3. Spearman correlation coefficients between annual anomalies of temperature and relative humidity at (a) 850 and (b) 700 hPa. The shading and outlining are as in Fig. 1.

North, central, and South America (hereinafter the Caribbean region) and the tropical western Pacific.

c. Statistical computations

Linear trends in the station and gridpoint 17-yr anomaly time series were removed to isolate better the interannual correlations. At each station and at each model grid point, Spearman nonparametric correlation coefficients (Wilks 1995) were calculated between pairs of the detrended annual and seasonal anomalies of q, RH, and T at each level. Spearman correlations, based on data ranks, are less affected by outliers in the data and can give a better indication of the strength of the relationship in the presence of nonlinearity than do Pearson correlation coefficients. A Spearman correlation coefficient of about 0.5 is significant at the 95% level for a sample size of 17. In summarizing the results, we focus on the large-scale patterns of the correlations, their sign, and statistical significance.

3. Results

a. Climatological features

The climatological structure of tropospheric temperature and water vapor as observed by radiosondes and as simulated by AGCMs has been documented in previous studies (Peixoto and Oort 1996; Ross and Elliott 1996a,b; Gaffen et al., 1992b, 1997). For the current study, we compared observed and simulated annually and regionally averaged *T*, *q*, and RH for the period of 1979–95. Differences between the model and observed regional averages are shown in Fig. 2. To avoid latitudinal or other sampling biases in the climatological comparison, the model data were linearly interpolated to the observed station locations and then regionally averaged. The models tend to simulate a colder troposphere except for the Tropics, which shows a warm bias, especially at 850 hPa. The exception is the YONU model, which is warmer in all areas. At mid- and high latitudes and over the Tropics, the models show 10%–20% higher RH than is observed. However, when the Pacific is examined separately, the RH bias is largely confined to the 850-hPa level and the models are drier than observed. Errors in *q* (not shown) are small at mid- and high latitudes but in the Tropics and Pacific are consistent with the RH biases in sign (1–3 g kg^{-1} moister over the Tropics and 1–4 g kg^{-1} drier at 850 hPa over the Pacific).

In contrast, Gaffen et al. (1997) found a general tendency for 28 AMIP-I models to have lower column-integrated water vapor *W* than was observed by radiosondes over North America and by satellites over the Pacific Ocean during the AMIP-I period of 1979–88. This disparity may reflect differences between the AMIP-I and AMIP-II simulations (i.e., many of the models have been substantially modified since AMIP I), differences in the observational data during the two periods, and uncertainty in observations. These biases do not affect the correlations, which are based on interannual variations about the mean.

b. Observed temperature–humidity correlations

Overall, we find predominantly positive correlations between observed *T* and *q* and negative correlations between *T* and RH, in general agreement with the zonal-average results of Sun and Oort (1995). This result implies that the warmer-than-normal years are moister (higher *q*) but less humid (lower RH) than normal and vice versa, with some notable regional and seasonal differences. Figure 1 shows annual *T*–*q* correlations at the 850- and 700-hPa levels; *T*–RH correlations are shown in Fig. 3. Comparable maps for the surface and 500-hPa levels closely resemble the maps for the nearest neighboring levels except where noted, but the most prominent differences are those between 850 and 700 hPa. In this section, we examine the correlation patterns in each geographical region in turn.

In the high-latitude region, most of the stations show large positive, statistically significant *T*–*q* correlations (Fig. 1), though the *T*–*q* relationship at 850 hPa is somewhat stronger than at 700 hPa. This result applies not only to the annual correlations but also to seasonal correlations. There can be substantial variability in the type of air mass in this region, and the influence of advection of relatively warm and moist airflow from the south or cold and dry flow from the north probably dominates these correlations, because both extremes contribute to a positive *T*–*q* correlation. The *T*–RH correlations (Fig. 3), although nearly all negative, are weaker than the *T*–*q* correlations, with only about one-half of the *T*–RH correlations exceeding 0.5 in magnitude at 850 hPa and fewer still at 700 hPa.

The observed correlation patterns in the midlatitude region are notable for the difference between the western and eastern U.S. patterns (Figs. 1 and 3). At eastern stations, correlations between *T* and *q* at 850 and 700 hPa are generally larger than those in the west, with more statistically significant positive correlations. In contrast, correlations between *T* and RH are generally negative but are largest in magnitude and statistically significant only in the western half of the midlatitude region at each of the four levels and in all seasons. Similar patterns are found at the surface and at 500 hPa.

This pattern of upper-air *T*–*q* correlations is consistent with the findings of Gaffen and Ross (1999) for U.S. surface temperature and humidity observations. The lower annual *T*–*q* correlations in the western United States are attributable to a tendency for negative *T*–*q* correlations in summertime in this region, except at 500 hPa, where summertime *T*–*q* correlations are weakly positive. Wintertime *T*–*q* correlations are positive and statistically significant at the majority of stations in the midlatitude regions. Thus, in the eastern United States, warmer-than-average summers are moister (but less humid) than average, but in the western United States, they are drier and less humid than average. As in high latitudes, the eastern United States, especially in winter, is influenced both by relatively warm and moist airflow from the south or by cold and dry flow from the north. In the western United States, the weak *T*–*q* correlation and strongly negative *T*–RH correlation (especially in summer) suggest that the relationship is related to variations in subsidence over the arid western United States. Note that subsidence conditions approximate the idealized scenario of constant *q*, and the near-zero *T*–*q* correlations and strong, negative *T*–RH correlations are consistent with that.

At low latitudes, we find differences between the Pacific and Caribbean regions (Fig. 1) and discuss them separately. The observed *T*–*q* correlations in the low-latitude Caribbean region are generally positive at the surface and at 850 hPa (Fig. 1), with negative values in the west as was seen in midlatitudes. At 700 (Fig. 1) and 500 hPa, *T*–*q* correlations retain this spatial pattern

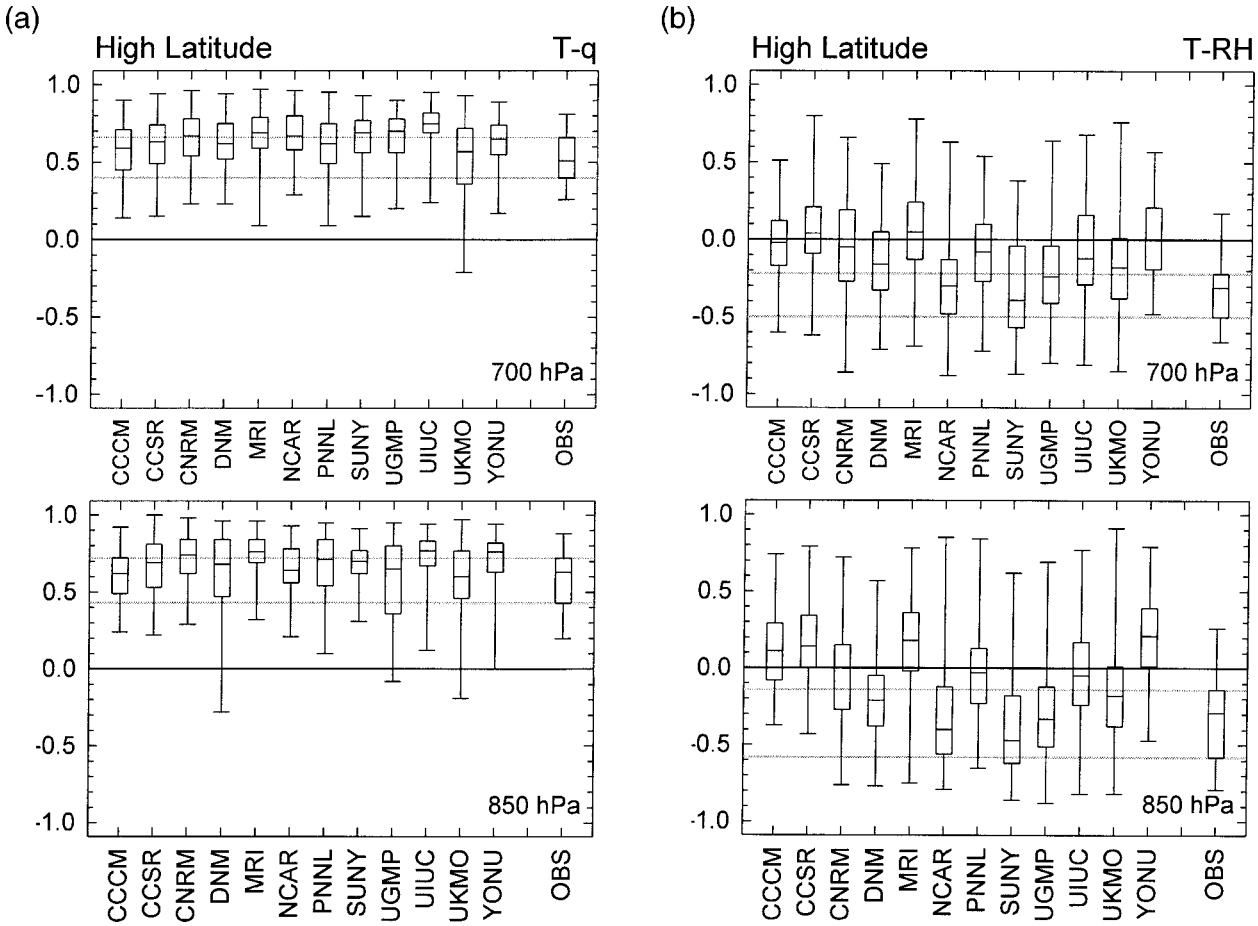

FIG. 4. Box-and-whisker plots of the distribution of Spearman correlation coefficients for 12 AGCMs and the observations in high latitudes at 700 (upper) and 850 (lower) hPa between simulated annual anomalies of (a) T and q and (b) T and RH. The whiskers run from the minimum to the maximum correlation, and the box shows the range of the innermost 50% of the correlations (i.e., from the 25th to the 75th percentile). The median is indicated by the horizontal line within each box. The horizontal gray lines, showing the observed innermost 50% of the correlations, are there to aid the comparison of the model ranges with the observations.

but are weaker, and most of the correlations are not statistically significant. The similarity of the correlations over the Caribbean with those at midlatitudes suggests a stronger continental influence than for tropical stations in the Pacific. Correlations between T and RH in this region are generally negative but not statistically significant at all four levels.

The situation is somewhat different in the low-latitude Pacific region, for which there is a distinct difference between large, statistically significant, positive annual T–q correlations at the surface and at 850 hPa (Fig. 1) and negative T–q correlations (generally small and not statistically significant) at 700 (Fig. 1) and 500 hPa. This vertical change in correlation is most prominent in wintertime, when the anticorrelation between T and q anomalies at 700 hPa is statistically significant at 10 of the 12 stations. The wintertime anomalies of T and q (not shown) indicate that the vertical change in T–q correlation results from decoupling and anticorrelation between 850- and 700-hPa T anomalies whereas q anomalies at these levels are vertically coherent. This decoupling varies interannually (it is most pronounced when T anomalies are largest) and seasonally (it is more prominent in winter and spring).

When this region experiences anomalously cold surface temperatures, it is likely associated with displacement of convection to other parts of the Tropics and thus enhanced subsidence in the region itself, attributable to variations in the location of the descending branches of the Walker and Hadley circulation cells. Enhanced subsidence may lead to positive free-tropospheric temperature anomalies (due to enhanced adiabatic warming) and negative free-tropospheric humidity anomalies (associated with the descent of air from anomalously high, cold, and dry convective regions). Within the boundary layer, negative temperature anomalies are associated with negative humidity anomalies (because oceanic boundary layer moisture content is largely temperature controlled).

Our results for low latitudes are similar to those of

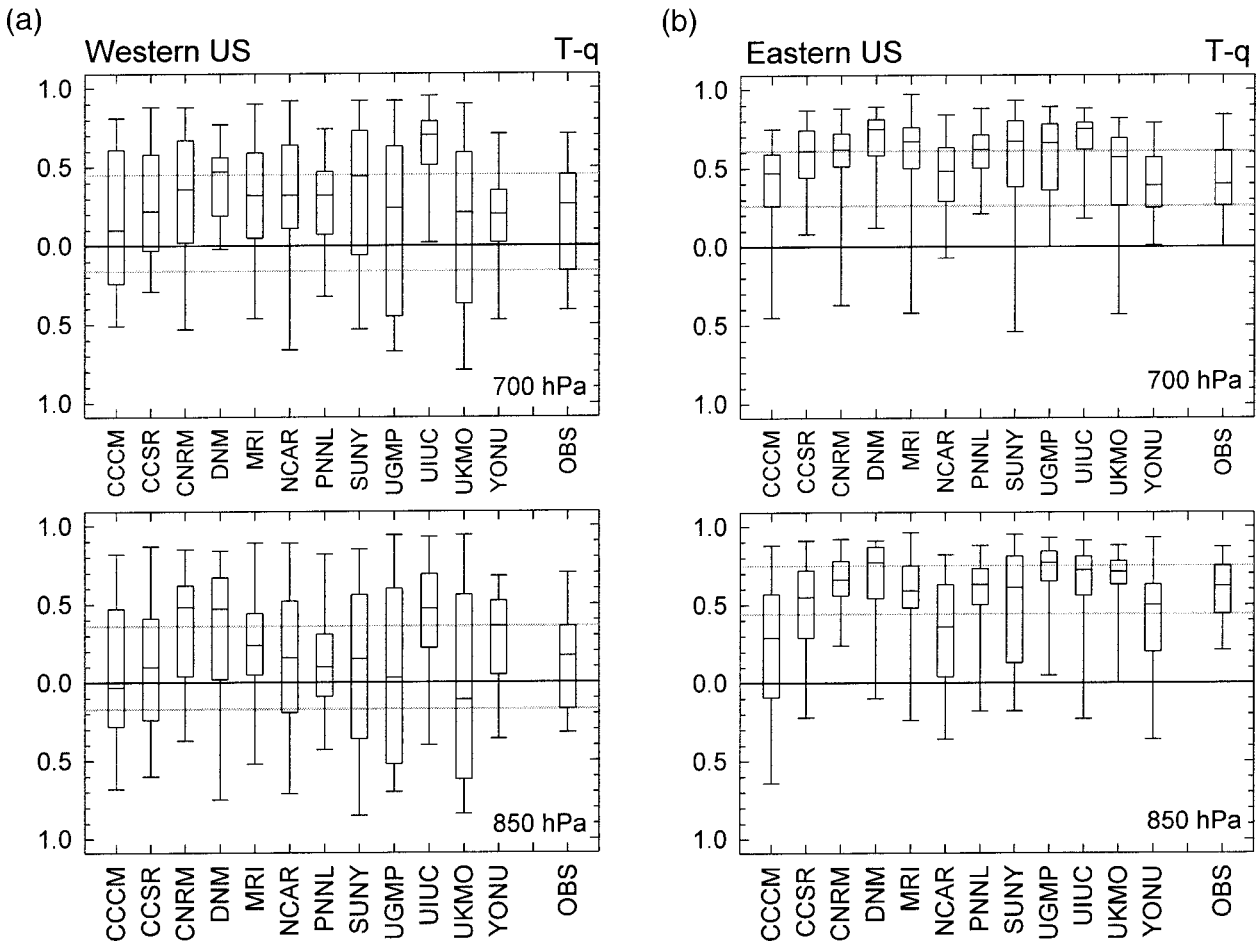

FIG. 5. Same as Fig. 4, but for the *T*–*q* correlations in the a) western and b) eastern United States.

Sun and Oort (1995) in so far as they can be compared. Although the zonally averaged tropical results of Sun and Oort (1995) do not show a change in sign between the 850- and 700-hPa *T*–*q* correlations as we find in our Pacific region, they show a minimum at 700 hPa that is consistent with a zonal average of correlations that vary geographically like the two low-latitude regions examined here.

c. Simulated temperature–humidity correlations

The observed relationships discussed above define features that the models should reproduce. Overall, the models successfully simulate the most basic of the observed correlation features: the predominantly positive *T*–*q* correlations and negative *T*–RH correlations. At 850 hPa, the percentage of points with positive *T*–*q* correlations in the models ranges from 73% to 94% as compared with an observed 88% of stations with positive *T*–*q* correlations. At 700 hPa, the models range from 69% to 91% as compared with an observed value of 76%. The models are a little less successful in reproducing as many negative *T*–RH correlations. Most models simulate negative *T*–RH correlations at less than 70% of the points at either level; the observed value is 84% and 88% at 850 and 700 hPa, respectively.

The simulated *T*–*q* correlations at 850 and 700 hPa are summarized for all 12 models and for each region in Figs. 4–8. The box-and-whisker plots indicate the range of correlation values, the median, and the interquartile range (25th–75th percentile) for each model. The corresponding observed range is shown on the right side of each plot. Positive *T*–*q* correlations at high latitudes (Fig. 4a) are represented well in the models, but, in many of the models, a substantial fraction of the modeled correlations are larger than observed. For example, the simulated median 700-hPa *T*–*q* correlations generally exceed 0.7, whereas observed correlations there show a lower median of 0.51.

The corresponding plots for simulated high-latitude *T*–RH correlations (Fig. 4b) show generally negative correlations, especially at 700 hPa, although there are more differences among the various models. When compared with the observations, many of the models show a larger fraction of positive or near-zero *T*–RH correlations. The models with the largest fraction of positive

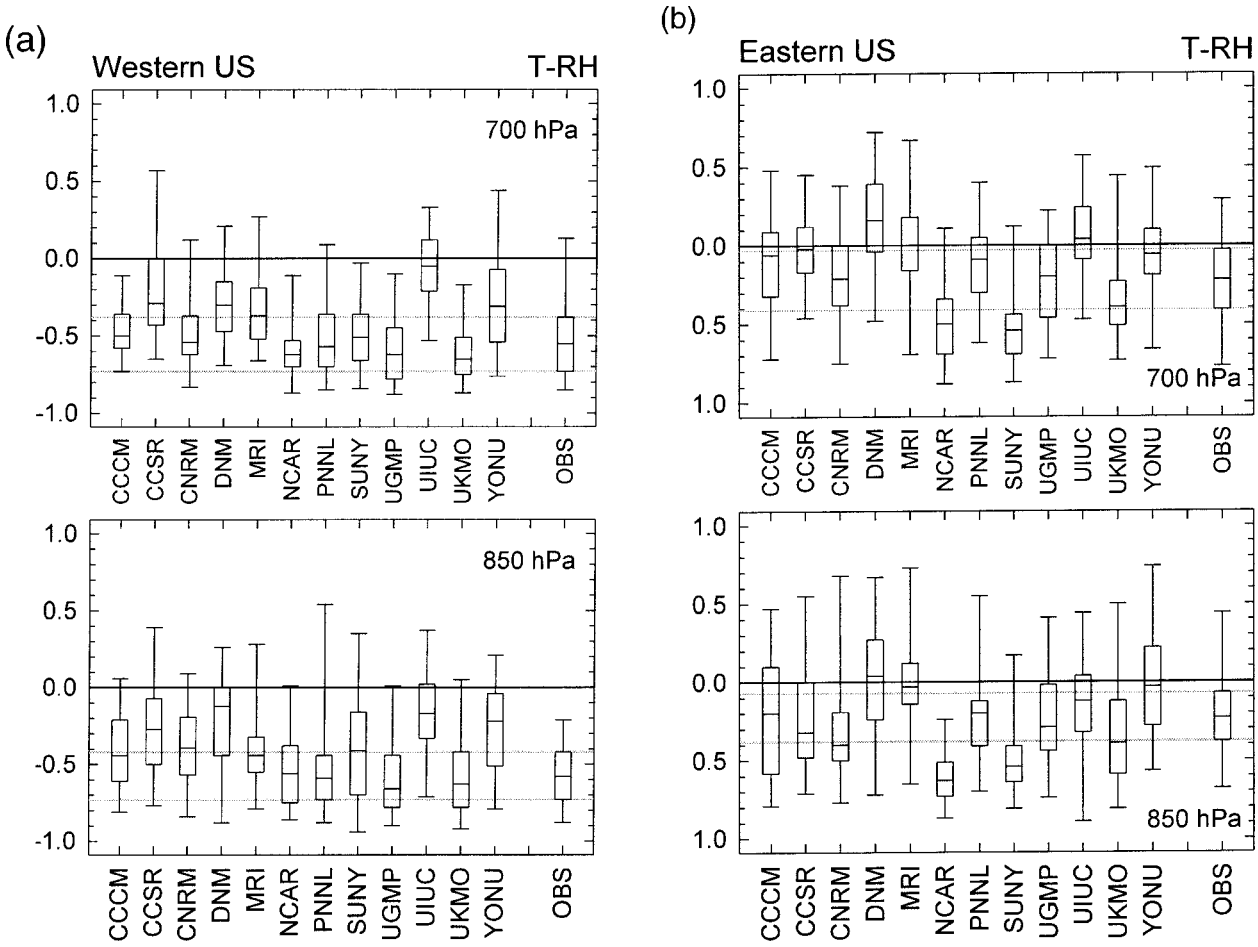

FIG. 6. Same as Fig. 5, but for the *T*–RH correlations.

T–RH correlations simulate a positive *T*–RH relationship over large portions of the high-latitude area, and all the models simulate an area of positive *T*–RH correlations (not shown) over southern Alaska and the Bering Sea at both 850 and 700 hPa. Observed correlations are generally negative (though near zero) in this area, so the models simulate a stronger-than-observed relationship between *T* and RH there. This area of positive *T*–RH correlation is most prominent in winter and least prominent in summer, perhaps suggesting an association with fluxes over sea ice.

In the midlatitude region, the observed pattern of positive *T*–*q* correlations over the eastern portion and weaker positive or even negative *T*–*q* correlations over the western portion is reproduced to some degree in most of the models (Fig. 5), although somewhat more clearly at 850 hPa. In a similar may, many models show larger negative *T*–RH correlations in the western midlatitudes (Fig. 6) than in the east as is observed, although a few models show little difference between the two regions.

Although the observed difference between the western and eastern U.S. correlations is usually discernable in the simulations, the strength of the *T*–*q* relationship in either region is not always accurately simulated. For example, at 700 hPa, stronger-than-observed positive correlations occur in many models over both the western and eastern United State. Discrepancies in the strength of the simulated midlatitude *T*–RH relationship are less consistent among the models. They tend to show weaker *T*–RH correlations than are observed over the western United States; over the eastern United States there are both stronger-than-observed and weaker-than-observed simulations. Thus, the models show varying degrees of success in simulating the observed *T*–*q* and *T*–RH relationships between eastern and western midlatitude North America.

For low latitudes, we focus on whether the models simulate the observed differences between the 850- and 700-hPa correlations in the Pacific region. The observations indicate that both the *T*–*q* and *T*–RH correlations are more negative at 700 than at 850 hPa. For the *T*–*q* correlations, nearly all the models do show evidence of this (i.e., higher medians at 850 than at 700 hPa in Fig. 7a), although the median 700-hPa *T*–*q* correlations of the models tend to be more positive than those observed. Also, a few models have median 850-hPa correlations

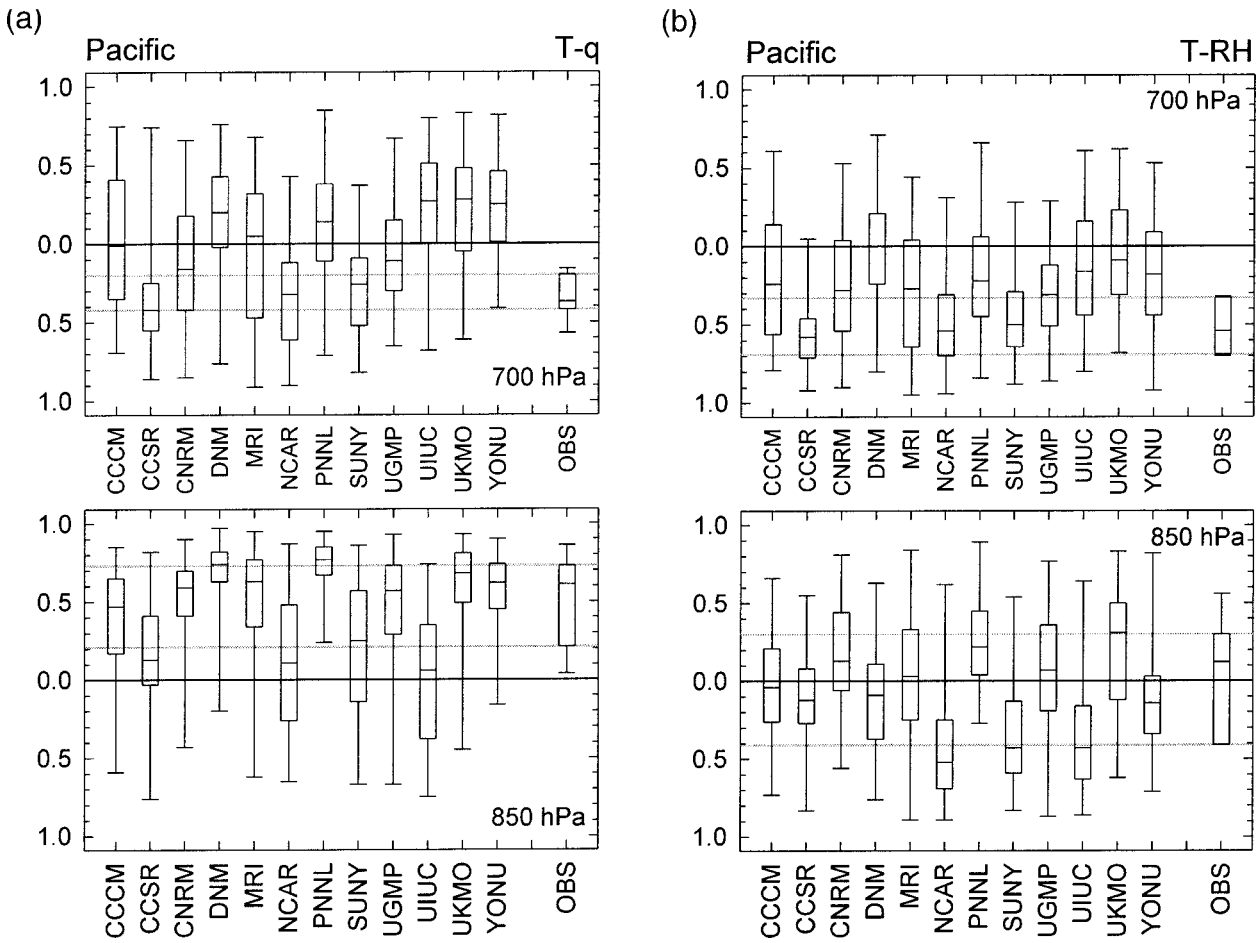

FIG. 7. Same as Fig. 4, but for the Pacific.

well below the observed median. Just over one-half of the models show *T*–RH median correlations (Fig. 7b) that are more negative at 700 than at 850 hPa, and the 700-hPa medians, although negative, are usually of smaller magnitude than those observed.

The *T*–*q* and *T*–RH correlation distributions for the low-latitude Pacific region are different from those in the other regions analyzed. As shown in Figs. 1 and 3, the observed Pacific 700-hPa *T*–*q* and *T*–RH correlations are generally both negative, in contrast with tropical locations over the Caribbean, for which *T*–*q* correlations are often positive. Nearly all of these AGCMs simulate *T*–*q* and *T*–RH correlations that are both positive and negative for both low-latitude regions (Figs. 7 and 8). However, several models have interquartile ranges that are entirely negative, similar to the observed range. At 850 hPa (Fig. 7a), the models are successful in simulating the generally positive *T*–*q* correlations over the Pacific, but a few models have median correlations that are considerably weaker (or negative) when compared with the observed. However, the observed Pacific distribution is based on relatively few stations, making these comparisons somewhat uncertain.

It is tempting to look for model attributes that might explain the different correlation results. The models have different horizontal and vertical resolutions (see Table 1) and physical parameterizations. However, previous studies using AMIP-I simulations, such as Gaffen et al. (1997) and Weare (1996), found it difficult to attribute simulation discrepancies from observations to specific differences in model physics or resolution. For example, to test whether higher vertical resolution improves the simulation one could compare the UGAMP and UKMO models (58 and 17 vertical levels, respectively), although the conclusions are compromised by other differences between the models. In fact, despite the difference in vertical levels, the UGAMP and UKMO models often show similar results. Thus, we hesitate to speculate as to the causes of particular models' correlation results as compared with observations.

4. Summary

This study has examined the correlations of seasonal and annual *T*, *q*, and RH anomalies in the lower troposphere (surface–500 hPa) during 1979–95, based on

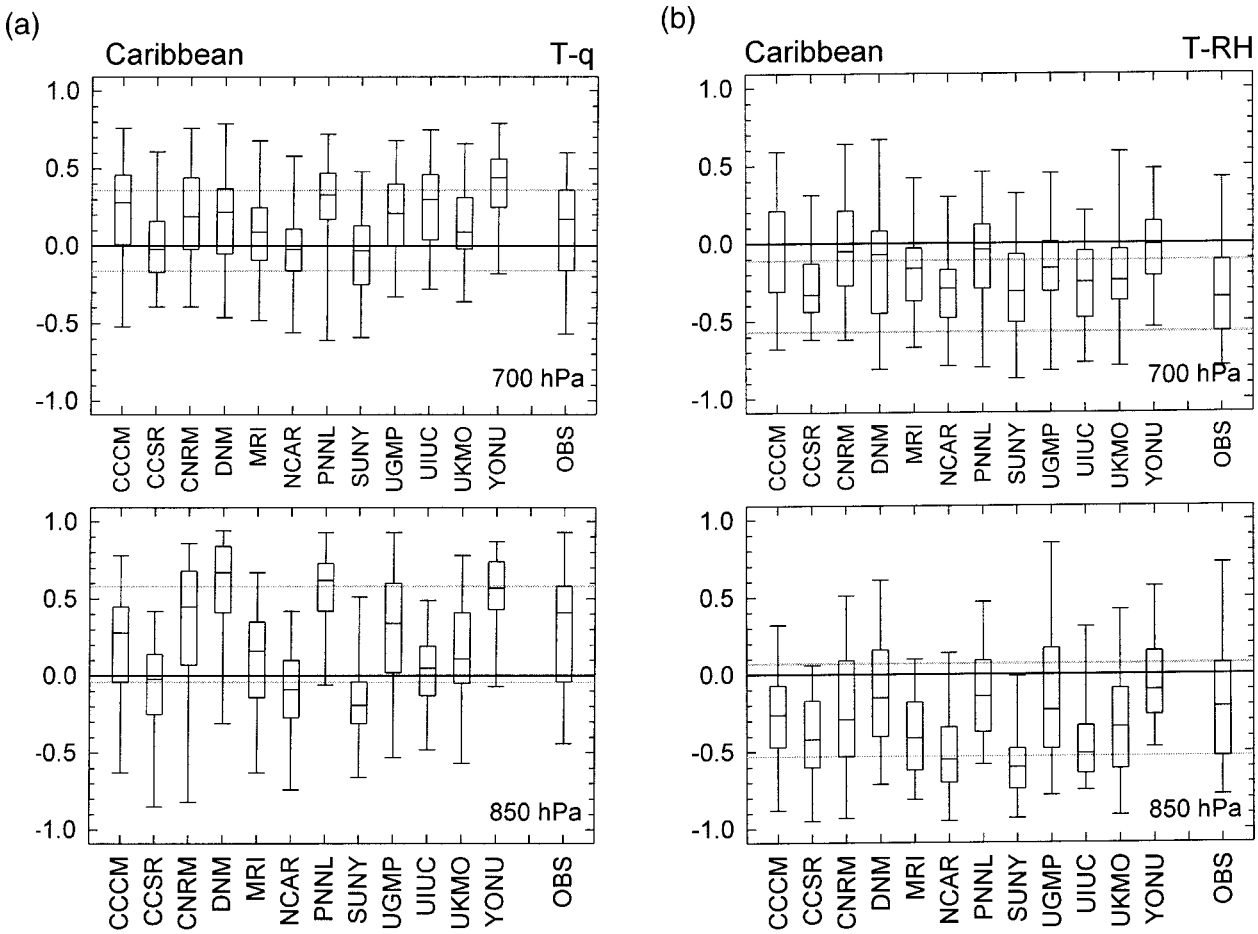

FIG. 8. Same as Fig. 4, but for the Caribbean.

radiosonde observations and as simulated by 12 AMIP-II AGCMs. Although correlation coefficients do not reveal the causes of the relationships, we have alluded to several possibilities above. Here we review the overall features of the distribution of correlations and speculate on their meanings. Our main findings are as follows.

1) Observed correlations between T and q at radiosonde stations in North America and U.S.-run stations in the western tropical Pacific and low-latitude Caribbean are predominantly positive, and those between T and RH are generally negative, so that warmer-than-normal years are moister (higher q) but less humid (lower RH) than normal. Thus, the most typical relationship is intermediate between either of two idealized scenarios (i.e., constant q or constant RH).
2) The observed positive T–q relationship is most consistent at high-latitude stations and over the eastern United States. This result is likely a reflection of the fact that flow from the north is likely to be characterized by low temperatures and less water vapor. The reverse is true for flow from the south where the Gulf of Mexico and the southern Atlantic are sources of both high temperatures and moisture for the eastern United States. Thus, flow from either direction contributes to the positive T–q relationship.
3) Over midlatitude North America and over low-latitude regions, we find regional variations in the relationship of temperature and humidity. In particular, near-zero or negative T–q correlations and negative T–RH correlations are found in the western United States at 700 hPa and below (especially in summer) and over the western tropical Pacific at 700 and 500 hPa (especially in winter). These relationships are consistent with the presence of subsidence over the Pacific and western United States. In contrast, over the Caribbean the free atmosphere is more closely coupled to the surface and the correlations reflect a more continental influence (i.e., similar to the midlatitudes).
4) Comparing the observed and modeled climatological behavior, we find the models show 10%–20% higher mean relative humidity than is observed at mid- and high latitudes and over the Tropics. However, over the Pacific region the models are drier than observed, mainly at the 850-hPa level. These biases occur

along with somewhat colder (1°–2°C) tropospheric temperatures, except over the Tropics for which there is an approximately 2°C warm bias.

5) Comparing the observed and simulated correlations, we find that the tendency for positive *T–q* correlations at high latitudes is represented well in the models, though nearly all models show a substantial fraction of correlations that are higher than observed. Also, all models show a higher fraction of positive *T*–RH correlations than is observed. These positive *T*–RH correlations are found primarily over southern Alaska and the Bering Sea and are most frequent in winter, suggesting possible connections with fluxes over sea ice.
6) The models are more disparate in their simulation of midlatitude variations in the *T–q* relationship. There is qualitative agreement in the pattern of weaker or negative *T–q* correlations in the western United States, but the simulated 700-hPa *T–q* relationship in either the western or eastern United States is often stronger than is observed. There is also a less consistent tendency for the *T*–RH relationship to be weaker than is observed.
7) The models are less successful in reproducing the observed differences in *T–q* correlations between the tropical western Pacific and the low-latitude Caribbean regions. The positive *T–q* correlations at 850 hPa over the Pacific are simulated fairly well by most models, but only a few models show the predominantly negative *T–q* relationship at 700 hPa that is observed. The *T*–RH relationship at 700 hPa over both tropical regions tends to be weaker than is observed.

By considering the correlations at station locations rather than in the zonal average, we have identified some regional variations in the observed relationship of temperature and humidity. That the tropical region is an area in which longitudinal variations occur is relevant when considering results from zonally averaged tropical studies.

Conclusions from previous model-versus-observed comparisons of the tropical temperature–humidity relationship using a single model have been limited by uncertainties regarding the particular model's sensitivity. This comparison of 12 simulations using the AMIP-II standardized experiment shows both areas of agreement and some discrepancies from observations. The most systematic discrepancies are found at 700 hPa, at which the simulated *T–q* relationships are more strongly positive than is observed and the simulated (negative) *T*–RH relationships tend to be weaker than is observed. The finding of some higher-than-observed tropical *T–q* correlations from the models is consistent with the zonally averaged tropical comparisons of Sun and Held (1996). The stronger-than-observed *T–q* relationship at high latitudes and over the eastern United States found here suggests the discrepancy is more widespread than in the Tropics. Furthermore, the tendency for some models to overestimate the correlation between temperature and specific humidity may imply that these models overestimate the lower-tropospheric water vapor feedback. If this is the case for models that depict the effects of increasing greenhouse gases, then they may be overestimating the temperature increases resulting from these greenhouse gas increases.

Acknowledgments. We are grateful to the Program for Climate Model Diagnosis and Intercomparison at Lawrence Livermore National Laboratory for making the simulations available for this project. We thank Sharon Le Duc, Richard Rosen, and the three anonymous reviewers for insightful comments and helpful suggestions. This work is part of AMIP-II diagnostic subproject No. 27: tropospheric humidity and meridional moisture fluxes.

REFERENCES

Bony, S., J.-P. Duvel, and H. Le Treut, 1995: Observed dependence of the water vapor and clear-sky greenhouse effect on sea surface temperature: Comparison with climate warming experiments. *Climate Dyn.,* **11,** 307–320.

Elliott, W. P., and D. J. Gaffen, 1991: On the utility of radiosonde humidity archives for climate studies. *Bull. Amer. Meteor. Soc.,* **72,** 1507–1520.

——, R. J. Ross, and B. Schwartz, 1998: Effects on climate records of changes in National Weather Service humidity processing procedures. *J. Climate,* **11,** 2424–2436.

Gaffen, D. J., 1996: A digitized metadata set of global upper-air station histories. NOAA Tech. Memo. ERL ARL-211, 38 pp.

——, and R. J. Ross, 1999: Climatology and trends in U.S. surface humidity and temperature. *J. Climate,* **12,** 811–828.

——, W. P. Elliott, and A. Robock, 1992a: Relationships between tropospheric water vapor and surface temperature as observed by radiosondes. *Geophys. Res. Lett.,* **19,** 1839–1842.

——, A. Robock, and W. P. Elliott, 1992b: Annual cycles of tropospheric water vapor. *J. Geophys. Res.,* **97,** 18 185–18 193.

——, R. D. Rosen, D. A. Salstein, and J. S. Boyle, 1997: Evaluation of tropospheric water vapor simulations from the Atmospheric Model Intercomparison Project. *J. Climate,* **10,** 1648–1661.

Garratt, J. R., D. M. O'Brien, M. R. Dix, J. M. Murphy, G. L. Stephens, and M. Wild, 1999: Surface radiation fluxes in transient climate simulations. *Global Planet. Change,* **20,** 33–55.

Hall, A., and S. Manabe, 1999: The role of water vapor feedback in unperturbed climate variability and global warming. *J. Climate,* **12,** 2327–2346.

Held, I. M., and B. J. Soden, 2000: Water vapor feedback and global warming. *Annu. Rev. Energy Environ.,* **25,** 441–475.

Hu, H., 1996: Water vapor and temperature lapse rate feedbacks in the mid-latitude seasonal cycle. *Geophys. Res. Lett.,* **23,** 1761–1764.

——, R. Oglesby, and B. Saltzman, 2000: The relationship between atmospheric water vapor and temperature in simulations of climate change. *Geophys. Res. Lett.,* **27,** 3513–3516.

Inoue, T., 1990: The relationship of sea surface temperature and water vapor amount to convection over the western tropical Pacific revealed from split window measurements. *J. Meteor. Soc. Japan,* **68,** 590–606.

Peixoto, J. P., and A. H. Oort, 1996: The climatology of relative humidity in the atmosphere. *J. Climate,* **9,** 3443–3463.

Randel, D. L., T. H. Vonder Haar, M. A. Ringerud, G. L. Stephens,

T. J. Greenwald, and C. L. Combs, 1996: A new global water vapor dataset. *Bull. Amer. Meteor. Soc.,* **77,** 1233–1246.

Ross, R. J., and W. P. Elliott, 1996a: Tropospheric water vapor climatology and trends over North America: 1973–93. *J. Climate,* **9,** 3561–3574.

——, and ——, 1996b: Tropospheric precipitable water: A radiosonde-based climatology. NOAA Tech. Memo. ERL ARL-219, 132 pp.

Stephens, G. L., 1990: On the relationship between water vapor over the oceans and sea surface temperature. *J. Climate,* **3,** 634–645.

Sun, D. Z., and A. H. Oort, 1995: Humidity–temperature relationships in the tropical troposphere. *J. Climate,* **8,** 1974–1987.

——, and I. M. Held, 1996: A comparison of modeled and observed relationships between interannual variations of water vapor and temperature. *J. Climate,* **9,** 665–675.

Wade, C. G., 1994: An evaluation of problems affecting the measurement of low relative humidity on the United States radiosonde. *J. Atmos. Oceanic Technol.,* **11,** 687–700.

Weare, B. C., 1996: Evaluation of the vertical structure of zonally averaged cloudiness and its variability in the Atmospheric Model Intercomparison Project. *J. Climate,* **9,** 3419–3431.

Wentz, F. J., and M. Schabel, 2000: Precise climate monitoring using complementary satellite data sets. *Nature,* **403,** 414–416.

Wilks, D. S., 1995: *Statistical Methods in the Atmospheric Sciences.* Academic Press, 467 pp.